

A continuum theory of multiphase mixtures for modelling biological growth

Harish Narayanan

University of Michigan

October 10th, 2007 – Ann Arbor, MI

Outline

- Introduction
- A Lagrangian perspective \Leftrightarrow Chapter 2
- Some representative numerical simulations \Leftrightarrow Chapter 3
- An Eulerian perspective \Leftrightarrow Chapter 4
- Some more representative numerical simulations \Leftrightarrow Chapter 5
- Conclusions

The motivating question

- *What constitutes an ideal environment for tissue growth?*



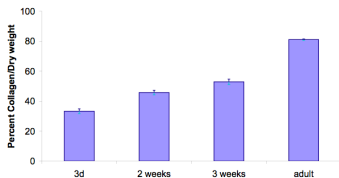
Engineered tendon constructs (Calve et al. [2004])

The motivating question

- *What constitutes an ideal environment for tissue growth?*



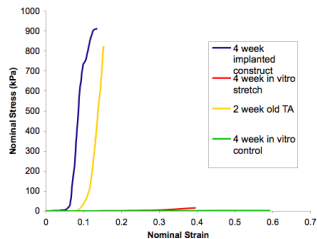
Engineered tendon constructs (Calve et al. [2004])



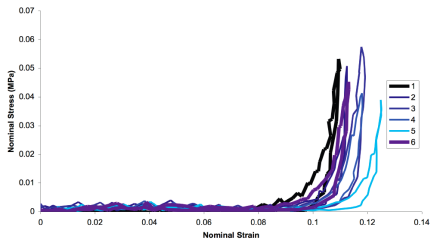
Increasing collagen concentration with age

- *Growth* involves an addition or depletion of mass

Some experimental observations

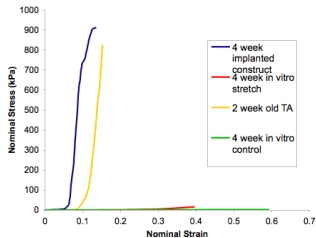


Uniaxial tensile response (Calve et al.)

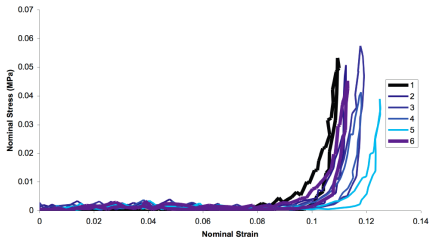


Response under cyclic load (Calve et al.)

Some experimental observations



Uniaxial tensile response (Calve et al.)



Response under cyclic load (Calve et al.)

- *What causes the tissue to behave in this manner?*
- Modelling of the coupled mechanics \Rightarrow Stiffness of the tissue and fluid transport \Rightarrow Nutrient transport \Rightarrow Tissue growth

Modelling approach

Classical balance laws enhanced via fluxes and sources

- Solid – Collagen, proteoglycans, cells
 - Extra cellular fluid
 - Undergoes transport relative to the solid phase
 - Dissolved solutes (sugars, proteins, . . .)
 - Undergo transport relative to the fluid
-
- Cowin and Hegedus [1976], Epstein and Maugin [2000]
 - Humphrey and Rajagopal [2002], *Garikipati et al. [2004]*
 - Loret and Simões [2005], Ateshian [2007]

Modelling approach

Classical balance laws enhanced via fluxes and sources

- Solid – Collagen, proteoglycans, cells
- Extra cellular fluid
 - Undergoes transport relative to the solid phase
- Dissolved solutes (sugars, proteins, . . .)
 - Undergo transport relative to the fluid

- Cowin and Hegedus [1976], Epstein and Maugin [2000]
- Humphrey and Rajagopal [2002], Gurtkipati *et al.* [2004]
- Loret and Simões [2005], Ateshian [2007]

Modelling approach

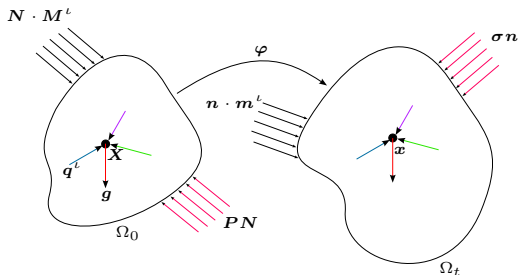
Classical balance laws enhanced via fluxes and sources

- Solid – Collagen, proteoglycans, cells
- Extra cellular fluid
 - Undergoes transport relative to the solid phase
- Dissolved solutes (sugars, proteins, . . .)
 - Undergo transport relative to the fluid

Some related literature:

- Cowin and Hegedus [1976], Epstein and Maugin [2000]
- Humphrey and Rajagopal [2002], *Garikipati et al. [2004]*
- Loret and Simões [2005], Ateshian [2007]

The governing equations—Lagrangian perspective



Reference quantities:

- ρ_0^l – Species concentration
- Π^l – Species production rate
- M^l – Species relative flux
- V^l – Species velocity
- g – Body force
- q^l – Interaction force
- P^l – Partial First Piola Kirchhoff stress

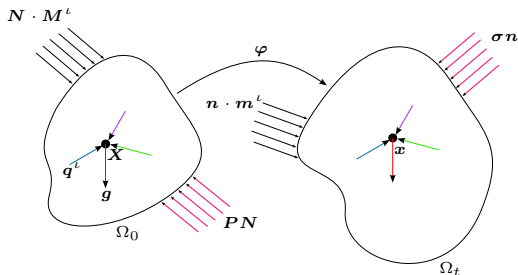
- Mass balance:

$$\frac{\partial \rho_0^l}{\partial t} = \Pi^l - \nabla_X \cdot M^l$$

- Momentum balance:

$$\rho_0^l \frac{\partial V^l}{\partial t} = \rho_0^l (g + q^l) + \nabla_X \cdot P^l - (\nabla_X V^l) M^l$$

The governing equations—Lagrangian perspective



Reference quantities:

- ρ_0^ℓ – Species concentration
- Π^ℓ – Species production rate
- M^ℓ – Species relative flux
- V^ℓ – Species velocity
- g – Body force
- q^ℓ – Interaction force
- P^ℓ – Partial First Piola Kirchhoff stress

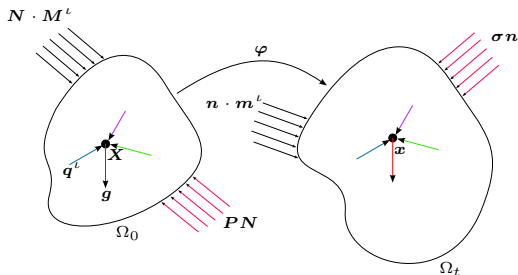
- Mass balance:

$$\frac{\partial \rho_0^\ell}{\partial t} = \Pi^\ell - \nabla_X \cdot M^\ell$$

- Momentum balance:

$$\rho_0^\ell \frac{\partial V^\ell}{\partial t} = \rho_0^\ell (g + q^\ell) + \nabla_X \cdot P^\ell - (\nabla_X V^\ell) M^\ell$$

The governing equations—Lagrangian perspective



Reference quantities:

- ρ_0^ℓ – Species concentration
- Π^ℓ – Species production rate
- M^ℓ – Species relative flux
- V^ℓ – Species velocity
- g – Body force
- q^ℓ – Interaction force
- P^ℓ – Partial First Piola Kirchhoff stress

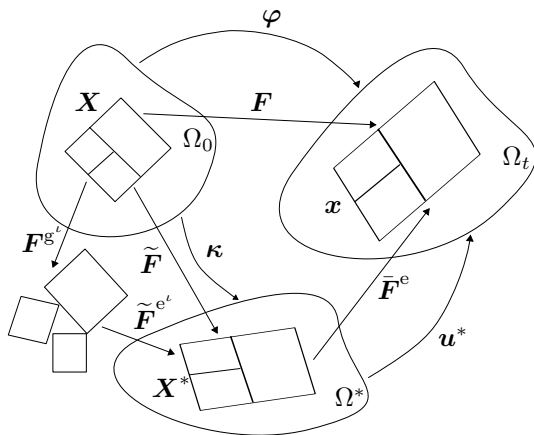
- Mass balance:

$$\frac{\partial \rho_0^\ell}{\partial t} = \Pi^\ell - \nabla_X \cdot M^\ell$$

- Momentum balance:

$$\rho_0^\ell \frac{\partial V^\ell}{\partial t} = \rho_0^\ell (g + q^\ell) + \nabla_X \cdot P^\ell - (\nabla_X V^\ell) M^\ell$$

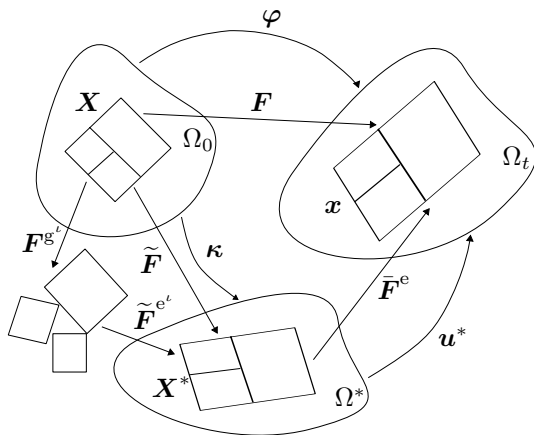
Growth kinematics



- $F = \bar{F}^e \tilde{F}^e F^{g^t}$; $F^{e^t} = \bar{F}^e \tilde{F}^e$; Internal stress due to \tilde{F}^e

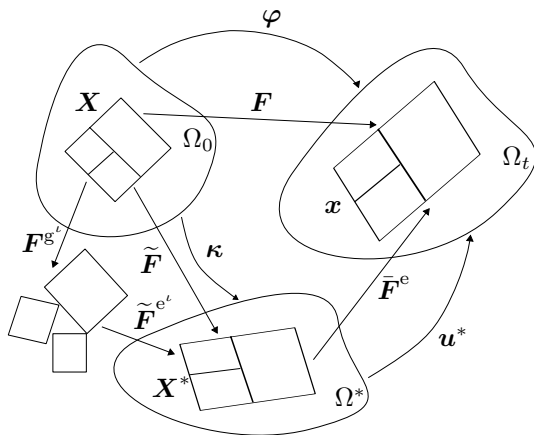
- Isotropic swelling due to growth: $F^{g^t} = \left(\frac{\rho_0^t}{\rho_{0,ini}^t} \right)^{\frac{1}{3}} \mathbf{1}$
- Saturation and swelling

Growth kinematics



- $F = \bar{F}^e \tilde{F}^{e^t} F^{g^t}$; $F^{e^t} = \bar{F}^e \tilde{F}^{e^t}$; Internal stress due to \tilde{F}^{e^t}
- Isotropic swelling due to growth: $F^{g^t} = \left(\frac{\rho_0^t}{\rho_{0\text{ini}}^t} \right)^{\frac{1}{3}} \mathbf{1}$
- Saturation and swelling

Growth kinematics



- $F = \bar{F}^e \tilde{F}^{e^t} F^{g^t}$; $F^{e^t} = \bar{F}^e \tilde{F}^{e^t}$; Internal stress due to \tilde{F}^{e^t}
- Isotropic swelling due to growth: $F^{g^t} = \left(\frac{\rho_0^t}{\rho_{0\text{ini}}^t} \right)^{\frac{1}{3}} \mathbf{1}$
- Saturation and swelling

Solving the balance equations in practice—A first pass

- Close the equations with thermodynamically-consistent constitutive relationships
 - Solid: Hyperelastic material, $\mathbf{P}^c = \rho_0^c \frac{\partial e^c}{\partial \mathbf{F}^{e^c}} \mathbf{F}^{g^{c-T}}$
Helmholtz free energy derived from entropic elasticity-based worm-like chain model
 - Fluid: Ideal, $\det(\mathbf{F}^{e^f})^{-1} \mathbf{P}^f \mathbf{F}^{e^{fT}} = h'(\rho^f) \mathbf{1}$

$$h(\rho^f) = \frac{1}{2} \kappa^f \left(\frac{\rho_{0\text{ini}}^f}{\rho^f} - 1 \right)^2$$

Solving the balance equations in practice—A first pass

- Close the equations with thermodynamically-consistent constitutive relationships
 - Solid: Hyperelastic material, $\mathbf{P}^c = \rho_0^c \frac{\partial e^c}{\partial \mathbf{F}^{e^c}} \mathbf{F}^{g^{c-T}}$
Helmholtz free energy derived from entropic elasticity-based worm-like chain model
 - Fluid: Ideal, $\det(\mathbf{F}^{e^f})^{-1} \mathbf{P}^f \mathbf{F}^{e^{fT}} = h'(\rho^f) \mathbf{1}$

$$h(\rho^f) = \frac{1}{2} \kappa^f \left(\frac{\rho_{0\text{ini}}^f}{\rho^f} - 1 \right)^2$$

- Sum species momentum balances to solve system-level balance law
 - Reduce number of partial differential equations by one
 - Avoid specification of \mathbf{q}^l , because $\sum_l (\rho_0^l \mathbf{q}^l + \Pi^l \mathbf{V}^l) = 0$

Solving the balance equations in practice—A first pass

- Close the equations with thermodynamically-consistent constitutive relationships
 - Solid: Hyperelastic material, $\mathbf{P}^c = \rho_0^c \frac{\partial e^c}{\partial \mathbf{F}^{ec}} \mathbf{F}^{g^{c-T}}$
Helmholtz free energy derived from entropic elasticity-based worm-like chain model
 - Fluid: Ideal, $\det(\mathbf{F}^{ef})^{-1} \mathbf{P}^f \mathbf{F}^{eT} = h'(\rho^f) \mathbf{1}$

$$h(\rho^f) = \frac{1}{2} \kappa^f \left(\frac{\rho_{0ini}^f}{\rho^f} - 1 \right)^2$$

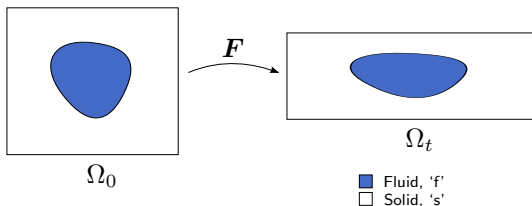
- Sum species momentum balances to solve system-level balance law
 - Reduce number of partial differential equations by one
 - Avoid specification of \mathbf{q}^l , because $\sum_l (\rho_0^l \mathbf{q}^l + \Pi^l \mathbf{V}^l) = 0$

- System-level motion determined, utilise a constitutive relationship to determine relative fluid flux

$$\mathbf{M}^f = \mathbf{D}^f \left(\rho_0^f \mathbf{F}^T \mathbf{g} + \mathbf{F}^T \nabla_X \cdot \mathbf{P}^f - \nabla_X (e^f - \theta \eta^f) \right)$$

Assumptions on the micromechanics

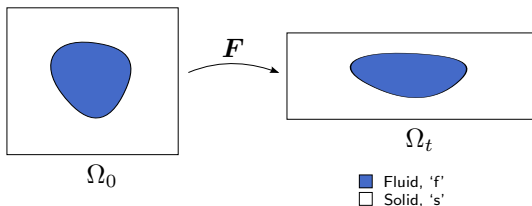
1. *Upper bound* model from strain homogenisation:



Pore structure deforms with the solid phase \Rightarrow Fluid-filled pore spaces see the overall deformation gradient

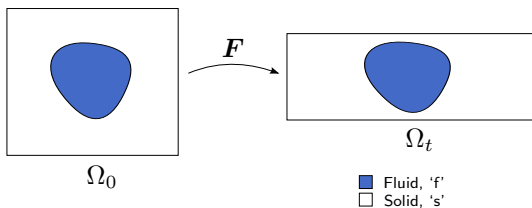
Assumptions on the micromechanics

1. *Upper bound* model from strain homogenisation:



Pore structure deforms with the solid phase \Rightarrow Fluid-filled pore spaces see the overall deformation gradient

2. *Lower bound* model from stress homogenisation:



Fluid pressure in the current configuration is the same as hydrostatic stress of the solid, $p^f = \frac{1}{3} \text{tr}[\sigma^s]$

3. More precise bounds exist, e.g. Idiart and Castañeda [2003]

An operator-splitting solution scheme

- Nonlinear projection methods to treat incompressibility
- Backward Euler for time-dependent mass balance
- Mixed method for stress/strain gradient-driven fluxes
- Large advective terms stabilised using SUPG

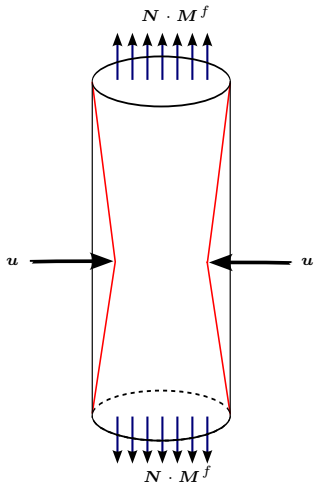
- Coupled implementation; staggered scheme

At each time step, repeat:

- Fixing the concentration fields, solve the mechanics problem for displacements, \mathbf{u}
- Fixing the displacement field, solve the mass transport problem for the concentration field, ρ^f

until both problems converge

Constriction of a tendon immersed in a bath



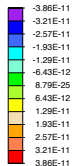
- Simulating a tendon immersed in a bath
- Constrict it radially to force fluid flow
- Biphasic model
 - Worm-like chain model for collagen
 - Ideal, nearly incompressible fluid
- Mobility from Han et al. [2000]

Evolution of the reference fluid concentration

Implications of the assumptions



Fluid flux (kg/m²/s)

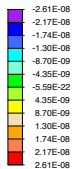


Time = 1.00E+00 s

Lower bound vertical fluid flux



Fluid flux (kg/m²/s)



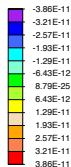
Time = 1.00E+00 s

Upper bound vertical fluid flux

Implications of the assumptions



Fluid flux (kg/m²/s)

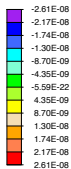


Time = 1.00E+00 s

Lower bound vertical fluid flux



Fluid flux (kg/m²/s)



Time = 1.00E+00 s

Upper bound vertical fluid flux

- Strength of coupling: $C = \frac{\delta p^f}{\frac{1}{3} \delta \text{tr}[\boldsymbol{\sigma}^s]}$
- Upper bound: $C \approx \frac{O(\kappa^f \delta \mathbf{F} : \mathbf{F}^{-\text{T}})}{O(\kappa^s \delta \mathbf{F} : \mathbf{F}^{-\text{T}})} = O\left(\frac{\kappa^f}{\kappa^s}\right) \gg 1$
- Lower bound: $C = 1$

A closer look at the convergence

Pass	Strongly coupled		Weakly coupled	
	Mechanics Residual	CPU (s)	Mechanics Residual	CPU (s)
1	2.138×10^{-02}	29.16	6.761×10^{-04}	28.5
	3.093×10^{-04}	55.85	1.075×10^{-04}	55.1
	2.443×10^{-06}	82.37	4.984×10^{-06}	81.8
	2.456×10^{-08}	109.61	1.698×10^{-08}	107.9
	4.697×10^{-14}	135.83	3.401×10^{-13}	134.1
	1.750×10^{-16}	163.18	1.1523×10^{-17}	161.1
2	5.308×10^{-06}	166.79	5.971×10^{-08}	192.5
	4.038×10^{-10}	193.36	4.285×10^{-11}	218.6
	1.440×10^{-14}	220.45	2.673×10^{-15}	246.1
	4.221×10^{-17}	247.04		
3	5.186×10^{-06}	250.62	2.194×10^{-09}	277.3
	3.852×10^{-10}	277.44	2.196×10^{-13}	304.2
	1.369×10^{-14}	304.16	1.096×10^{-17}	331.6
	4.120×10^{-17}	331.47		
4	5.065×10^{-06}	335.16	8.160×10^{-11}	363.2
	3.674×10^{-10}	362.24	7.923×10^{-15}	390.2
	1.300×10^{-14}	388.79		
	4.021×10^{-17}	416.08		
5	4.948×10^{-06}	419.59	3.078×10^{-12}	421.4
	3.503×10^{-10}	446.24	3.042×10^{-16}	448.6
	1.236×10^{-14}	473.20		
	3.924×10^{-17}	500.85		
6	4.832×10^{-06}	504.65	1.179×10^{-13}	479.9
	3.340×10^{-10}	531.28	1.291×10^{-17}	507.0
	1.174×10^{-14}	558.17		
	3.829×10^{-17}	585.27		

Swelling of a tendon immersed in a bath

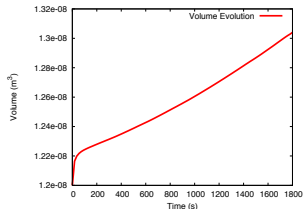
First order rate law:

$$\Pi^f = -k^f(\rho^f - \rho_{ini}^f),$$

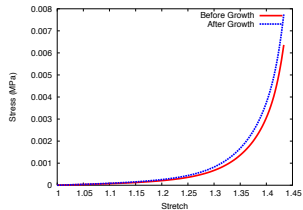
$$\Pi^c = -\Pi^f$$

Collagen concentration evolution

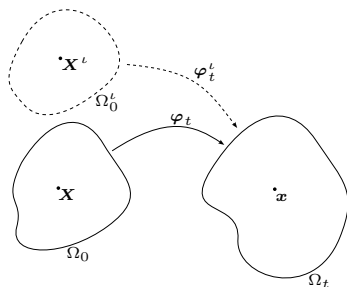
Volume evolution curve



Stress-extension curves



The governing equations—Eulerian perspective



Current quantities:

- ρ^l – Species concentration
- π^l – Species production rate
- \mathbf{m}^l – Species total flux
- \mathbf{v}^l – Species velocity
- \mathbf{g} – Body force
- \mathbf{q}^l – Interaction force
- $\boldsymbol{\sigma}^l$ – Partial Cauchy stress

- The notion of a deformation gradient is unnatural for the fluid

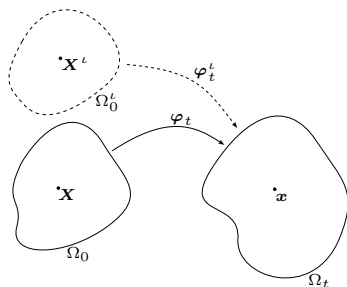
- Mass balance:

$$\frac{\partial \rho^l}{\partial t} = \pi^l - \nabla_x \cdot \mathbf{m}^l$$

- Momentum balance:

$$\rho^l \frac{\partial \mathbf{v}^l}{\partial t} = \rho^l (\mathbf{g}^l + \mathbf{q}^l) + \nabla_x \cdot \boldsymbol{\sigma}^l - (\nabla_x \mathbf{v}^l) \mathbf{m}^l$$

The governing equations—Eulerian perspective



Current quantities:

- ρ^l – Species concentration
- π^l – Species production rate
- \mathbf{m}^l – Species total flux
- \mathbf{v}^l – Species velocity
- \mathbf{g} – Body force
- \mathbf{q}^l – Interaction force
- $\boldsymbol{\sigma}^l$ – Partial Cauchy stress

- The notion of a deformation gradient is unnatural for the fluid

- Mass balance:

$$\frac{\partial \rho^l}{\partial t} = \pi^l - \nabla_x \cdot \mathbf{m}^l$$

- Momentum balance:

$$\rho^l \frac{\partial \mathbf{v}^l}{\partial t} = \rho^l (\mathbf{g}^l + \mathbf{q}^l) + \nabla_x \cdot \boldsymbol{\sigma}^l - (\nabla_x \mathbf{v}^l) \mathbf{m}^l$$

Returning to the dissipation inequality

Upon combining the balance of energy and the entropy inequality at uniform, constant temperature:

$$\sum_{\iota} \left(\rho^{\iota} \dot{\psi}^{\iota} - \boldsymbol{\sigma}^{\iota} : \text{grad}(\mathbf{v}^{\iota}) + \rho^{\iota} \text{grad}(\psi^{\iota}) \cdot \mathbf{v}^{\iota} \right) + \sum_{\iota} \left(\rho^{\iota} \mathbf{q}^{\iota} \cdot \mathbf{v}^{\iota} + \pi^{\iota} \left(\psi^{\iota} + \frac{1}{2} \|\mathbf{v}^{\iota}\|^2 \right) \right) \leq 0$$

- A viscoelastic solid; A Newtonian fluid
- Effects of the stress state on tissue growth
- Frictional interaction forces
- Energy-dependent mass source terms

Energy-dependent mass source terms

$$\sum_{\iota} \pi^{\iota} \left(\psi^{\iota} + \frac{1}{2} \|\mathbf{v}^{\iota}\|^2 \right) \leq 0, \quad \pi^f = 0 \Rightarrow$$

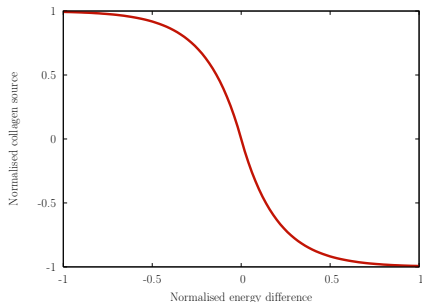
For e.g., $\pi^c = -\kappa^c A$, or

$$\pi^c = \epsilon \kappa^c (\exp[-\epsilon U A] - 1)$$

where

$$A = \left(\psi^c + \frac{1}{2} \|\mathbf{v}^c\|^2 - \psi^s - \frac{1}{2} \|\mathbf{v}^s\|^2 \right),$$

$$\epsilon = \text{sign}(A), \quad U > 0 \text{ and } \kappa^c \geq 0$$



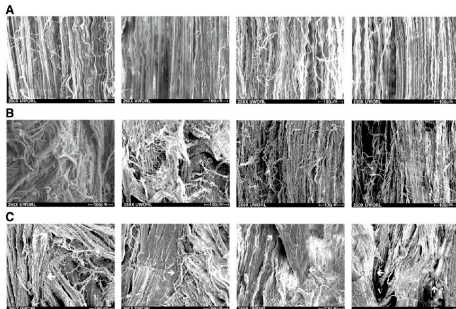
A thermodynamically-motivated collagen source

The thermodynamics indicates that the collagen source should be positive when the solute is more energetic

Effects of the stress state on tissue growth

$$-\mathbf{F}^{eT} \mathbf{P}^c : \dot{\mathbf{F}}^g \leq 0 \Rightarrow \dot{\mathbf{F}}^g = \lambda \mathbf{F}^{eT} \mathbf{P}^c, \quad \lambda \geq 0$$

i.e., Incremental changes in the growth deformation gradient align with the partial first Piola-Kirchhoff stress



Hindlimb unloading alters ligament healing (Provenzano et al. [2003])

Solving the balance laws in practice—Reprise

- Impose the “detailed” balance of momentum instead
- Close the equations by specifying constitutive relationships for stress and momentum transfer terms arising from dissipation inequality: $\rho^c \mathbf{q}^c = -\rho^f \mathbf{q}^f = -\mathbf{D}^{fc} (\mathbf{v}^c - \mathbf{v}^f)$

Solving the balance laws in practice—Reprise

- Impose the “detailed” balance of momentum instead
- Close the equations by specifying constitutive relationships for stress and momentum transfer terms arising from dissipation inequality: $\rho^c \mathbf{q}^c = -\rho^f \mathbf{q}^f = -\mathbf{D}^{fc} (\mathbf{v}^c - \mathbf{v}^f)$
- Solve fluid equations in the current configuration \Rightarrow No notion of any deformation gradient besides \mathbf{F}
- Assume intrinsic incompressibility and impose tissue saturation:

$$\frac{(\rho_0^c/J)}{\bar{\rho}^c} + \frac{\rho^f}{\bar{\rho}^f} = 1$$

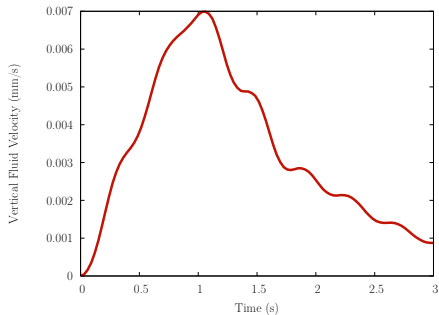
Solving the balance laws in practice—Reprise

- Impose the “detailed” balance of momentum instead
- Close the equations by specifying constitutive relationships for stress and momentum transfer terms arising from dissipation inequality: $\rho^c \mathbf{q}^c = -\rho^f \mathbf{q}^f = -\mathbf{D}^{fc} (\mathbf{v}^c - \mathbf{v}^f)$
- Solve fluid equations in the current configuration \Rightarrow No notion of any deformation gradient besides \mathbf{F}
- Assume intrinsic incompressibility and impose tissue saturation:
$$\frac{(\rho_0^c/J)}{\bar{\rho}^c} + \frac{\rho^f}{\bar{\rho}^f} = 1$$
- Strain energy function for the elastic portion of the response of the solid collagen is the model of Mooney and Rivlin:
$$\hat{\psi}^c(\mathbf{C}^e) = \sum_{i,j=0}^n C_{ij} (I_1 - 3)^i (I_2 - 3)^j$$
- Fluid is ideal; Pressure serves as a Lagrange multiplier to impose the saturation constraint

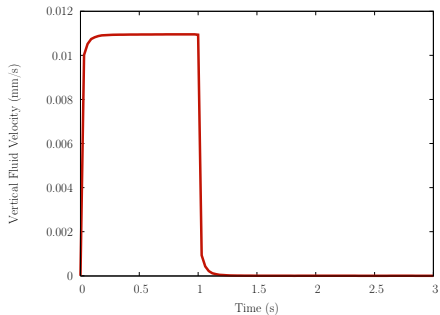
The swelling balloon

The constricted tissue

Contrasting the dynamic and quasistatic solution

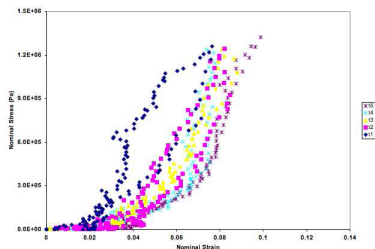


Dynamic evolution of the vertical fluid velocity



Quasistatic evolution of the vertical fluid velocity

Tests using parameters for realistic soft tissue

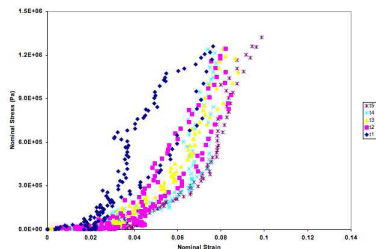


Mechanical response of a ligament (Ma et al.)

Parameter	Value (GPa)
C_{10}	0
C_{01}	0
C_{20}	0.54434
C_{11}	0
C_{02}	0.54714
C_{30}	1.83688
C_{21}	1.19985
C_{12}	10.6863
C_{03}	38.3875

- Friction coefficient tensor fit to Swartz et al. [1999]
 $D^{fc} = D \mathbf{1} = 1.037 \mathbf{1} \text{ MPa.s.mm}^{-2}$
- Solid collagen comprises 30% of the total mass of the mixture

Tests using parameters for realistic soft tissue

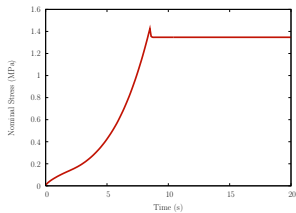


Mechanical response of a ligament (Ma et al.)

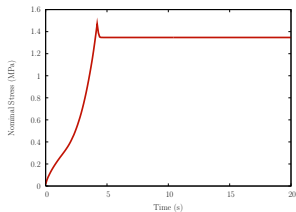
Parameter	Value (GPa)
C_{10}	0
C_{01}	0
C_{20}	0.54434
C_{11}	0
C_{02}	0.54714
C_{30}	1.83688
C_{21}	1.19985
C_{12}	10.6863
C_{03}	38.3875

- Friction coefficient tensor fit to Swartz et al. [1999]
 $D^{fc} = D \mathbf{1} = 1.037 \mathbf{1} \text{ MPa.s.mm}^{-2}$
- Solid collagen comprises 30% of the total mass of the mixture

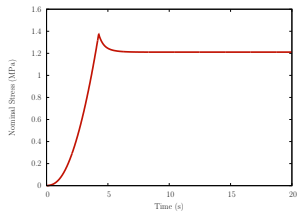
Stress relaxation



Poroelastic model, $\dot{\epsilon} = 0.01$ Hz, $D = 1.037$ MPa.s.mm⁻²

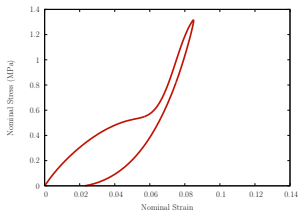


Poroelastic model, $\dot{\epsilon} = 0.02$ Hz, $D = 1.037$ MPa.s.mm⁻²

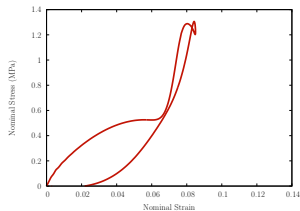


Viscoelastic model, $\dot{\epsilon} = 0.02$ Hz, $\tau = 0.3$ s

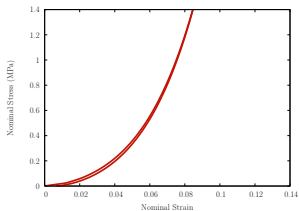
Hysteresis in the cyclic stress-strain response



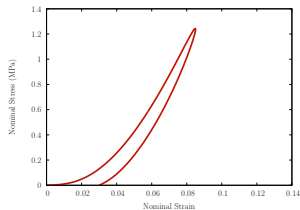
Poroelastic model, $\bar{\epsilon} = 0.01$ Hz, $D = 1.037$ MPa.s.mm⁻²



Poroelastic model, $\bar{\epsilon} = 0.01$ Hz, $D = 10.37$ MPa.s.mm⁻²



Poroelastic model, $\bar{\epsilon} = 0.001$ Hz, $D = 1.037$ MPa.s.mm⁻²



Viscoelastic model, $\dot{\epsilon} = 0.01$ Hz, $\tau = 0.3$ s

The physics of growing tumours

- Compressive solid stress along a given direction restricts the in vitro growth of tumours along that direction (Helmlinger et al. [1997])
- Solid comprised of an extra-cellular matrix (ECM) and tumour cells capable of moving with respect to this matrix
- Balance of mass with a uniform source
- Isotropic (plane strain) swelling associated with this growth:

$$F^{g^c} = \begin{pmatrix} \left(\frac{\rho_0^c}{\rho_{0,\text{ini}}^c}\right)^{1/2} & 0 & 0 \\ 0 & \left(\frac{\rho_0^c}{\rho_{0,\text{ini}}^c}\right)^{1/2} & 0 \\ 0 & 0 & 1 \end{pmatrix}$$

The physics of growing tumours

- Compressive solid stress along a given direction restricts the in vitro growth of tumours along that direction (Helmlinger et al. [1997])
- Solid comprised of an extra-cellular matrix (ECM) and tumour cells capable of moving with respect to this matrix
- Balance of mass with a uniform source
- Isotropic (plane strain) swelling associated with this growth:

$$\mathbf{F}^{\text{g}^c} = \begin{pmatrix} \left(\frac{\rho_0^c}{\rho_{0\text{ini}}^c}\right)^{1/2} & 0 & 0 \\ 0 & \left(\frac{\rho_0^c}{\rho_{0\text{ini}}^c}\right)^{1/2} & 0 \\ 0 & 0 & 1 \end{pmatrix}$$

Kinematic swelling along with growth

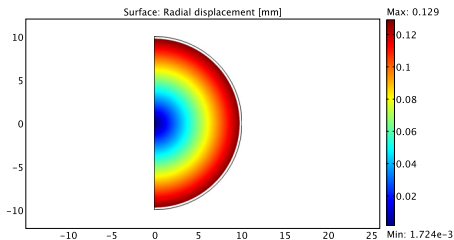
A constraining wall and soft contact mechanics

The mechanics of the cells

Total solid stress:

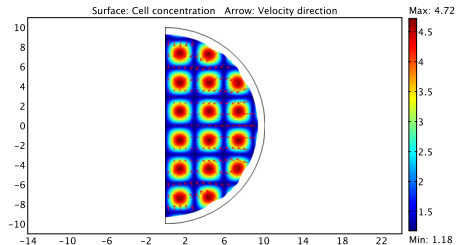
$$\boldsymbol{\sigma}^c = \underbrace{\frac{1}{J} \frac{\rho_0^c}{\tilde{\rho}_0^c} \frac{\partial \hat{\psi}^c}{\partial \mathbf{F}} \mathbf{F}^T}_{\text{Passive}} + \underbrace{\tau \rho^c \rho^{\text{cell}} (N - \rho^{\text{cell}})}_{\text{Active}} \mathbf{1}$$

Surface: Radial displacement [mm]



Homogeneous inward pull

Surface: Cell concentration Arrow: Velocity direction



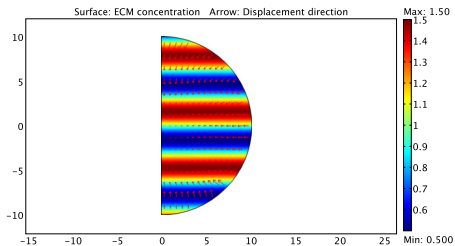
Heterogeneous inward pull

Modelling choices based on Namy et al. [2004]

Transport of the cells

Mass flux of the cells:

$$\rho^{\text{cell}} \mathbf{v}^{\text{cell}} = \underbrace{h \rho^{\text{cell}} \text{grad}(\rho^{\text{c}})}_{\text{Haptotactic flux}} - \underbrace{D^{\text{cell}} \text{grad}(\rho^{\text{cell}})}_{\text{Cell diffusion}}$$



Non-uniform matrix concentration

Diffusion and proliferation of the cells

Proliferating cells undergoing haptotaxis

Coupling the phenomena

A growing tumour constrained by a wall

Concluding remarks

The computational framework furnishes a powerful tool that can be tailored to answer specific questions pertinent to:

- Viscoelastic aspects of the mechanical response of growing tendons under different loading conditions
- Quantitative investigations of the efficacy of drugs based on how they are administered
- Understanding the cellular processes associated with tumour growth
- Mechanics of inflating automobile tyres!
- Ongoing work includes:
 - Extending the computational formulation to a viscoelastic solid and a viscous fluid
 - Introducing nonlinear viscoelasticity
 - Exploring the experimental literature to directly correlate some of the thermodynamic findings

Concluding remarks

The computational framework furnishes a powerful tool that can be tailored to answer specific questions pertinent to:

- Viscoelastic aspects of the mechanical response of growing tendons under different loading conditions
- Quantitative investigations of the efficacy of drugs based on how they are administered
- Understanding the cellular processes associated with tumour growth
- Mechanics of inflating automobile tyres!
- Ongoing work includes:
 - Extending the computational formulation to a viscoelastic solid and a viscous fluid
 - Introducing nonlinear viscoelasticity
 - Exploring the experimental literature to directly correlate some of the thermodynamic findings

Acknowledgements

- Krishna Garikipati, Ellen Arruda, Karl Grosh, Trachette Jackson
- Sarah Calve, Joe Olberding, Devin O'Connor, Fatima Syed-Picard
- National Science Foundation, Sandia National Labs, My parents, Mechanical Engineering Department